Energy Advances

ROYAL SOCIETY OF CHEMISTRY

REVIEW ARTICLE

View Article Online
View Journal | View Issue

Cite this: *Energy Adv.*, 2026, 5, 249

Modification strategies and recent advances of sodium titanate anode materials for enhanced electrochemical performance in sodium ion batteries

W. P. U. S. Wickramarathna and N. P. W. Rathuwadu *

Sodium-ion batteries (SIBs) are prospective next-generation alternatives to lithium-ion batteries (LIBs). Recently, most research has focused on the sodium titanate (NTO) structure as a possible anode with a low operating potential for SIBs. Furthermore, NTO has excellent stability and safety, and a suitable sodium storage capability. Although there are various types of NTOs, such as $NaTiO_2$, $Na_4Ti_5O_{12}$, $Na_2Ti_6O_{13}$, and $Na_2Ti_3O_7$, the most common NTO with a low operating voltage of 0.3 V *vs.* Na/Na^+ is layered $Na_2Ti_3O_7$. However, the sluggish ion insertion/extraction kinetics, substantial lattice expansion, low electronic conductivity, and the low Na^+ ion diffusion limit the electrochemical performance of NTO. To address these challenges, several modification techniques have been developed, including nanostructure engineering, ion doping, the incorporation of carbon-based composites, carbon coating, and other surface modification techniques. Herein, the types of NTOs and the corresponding modification strategies that enhance the electrochemical performance of NTO anodes are outlined. The effects of these modification strategies on the NTO structure and their resulting electrochemical improvements are systematically summarized. Nanostructure engineering is widely employed in NTO anodes because the large surface area of the nanosized structures will accelerate surface processes, thereby improving the electrochemical properties. SIB research for stationary energy storage will be substantially aided by the use of modified NTO anode materials.

Received 2nd November 2025,
Accepted 20th January 2026

DOI: 10.1039/d5ya00317b

rsc.li/energy-advances

1. Introduction

Due to the world's increasing energy consumption and persistent reliance on fossil fuels, the demand for these resources remains significantly high. In addition to raising prices, this demand is contributing to the potential depletion of fossil fuel reserves. This has prompted researchers to investigate and employ alternative and renewable energy sources such as wind, solar, hydropower, geothermal, and nuclear energies. For the continuous and effective utilization of alternative and renewable energy sources, developing suitable energy conversion and storage technologies, such as supercapacitors and rechargeable batteries, is essential.[1] Lithium-ion batteries (LIBs), the most common type of rechargeable battery, have dominated the portable device rechargeable battery market for over 20 years and are still the best option for portable electronic devices, electric vehicles, and hybrid electric vehicles[2] due to their high energy density, high coulombic efficiency, and low self-discharge characteristics.[3] However, due to the limited abundance of LIB raw materials, such as lithium, cobalt, nickel, and manganese, it is challenging to synthesize sufficient LIBs to meet the global demand. Moreover, the extraction and processing of Li sources and the disposal of LIBs create environmental impacts.[4]

Sodium-ion batteries (SIBs) have gained attention as a cost-effective substitute for LIBs. In contrast to Li, Na is one of the most abundant elements in the Earth's crust and has a suitable standard reduction potential $\left(E^0_{(Na^+/Na)} = -2.71\ V\right)$, which is 330 mV higher than that of Li $\left(E^0_{(Li^+/Li)} = -3.04\ V\right)$. Considering similar chemistry based on similar redox properties (reversible intercalation/deintercalation) and working principles ("rocking chair" mechanism), SIBs serve as ideal alternatives to LIBs.[5,6] However, Na^+ is larger and heavier than Li^+, and it lowers the packing density within the electrode, consequently lowering the overall energy density. Due to the larger ionic radius of Na^+ than that of Li^+, it also faces challenges in terms of insertion into and extraction from the electrode material.[7,8] Moreover, the larger size of Na^+ results in sluggish kinetics and considerable volume expansion. Therefore, the conventional

Institute for Combinatorial Advanced Research & Education, General Sir John Kotelawala Defence University, Ratmalana, Sri Lanka.
E-mail: npwrathu@gmail.com

electrode materials used in LIBs, such as graphite anodes and layered oxide cathodes, are not well-suited for SIBs.[9] As a result, the development of more suitable electrode materials has become imperative.

In SIBs, the anode plays a critical role in determining the overall energy density, rate capability, and cycling stability of the cell. Efficient Na^+ storage at the anode ensures high reversible capacity and minimal volume expansion during cycling. Moreover, the anode material governs the formation and stability of the solid electrolyte interphase (SEI), which is essential for long-term performance and safety.[10] Accordingly, carbonaceous materials,[11,12] alloying materials,[13,14] and metal oxides[15–17] have been investigated as potential anode materials for SIBs. Hard carbon, a non-graphitizable carbon-based material, is the most common anode material in SIBs. However, there are limitations in hard carbon, including low first-cycle coulombic efficiency, large irreversible capacity loss, moderate cycle stability, poor rate performance, and safety issues due to sodiated hard carbon.[18] Recently, a variety of titanium-based oxide compounds have been explored as promising anode materials due to their low cost, minimal toxicity, chemical stability, and environmental friendliness.[19] In Na/Ti-containing oxides, such as sodium titanates (NTOs), the titanium redox couple (Ti^{4+}/Ti^{3+}) provides suitable electrochemical activity, enabling their use as battery electrodes. NTOs have the potential to offer an appropriate insertion potential, higher initial coulombic efficiency, minimal irreversible capacity loss, and faster rate performance, while guaranteeing exceptional structural stability and safety, ensuring the sustained functionality of SIBs.[6]

In this review, we present a comprehensive discussion on NTO anode materials, emphasizing recent advances in their modification strategies aimed at enhancing electrochemical performance. This work uniquely focuses on how different modification approaches, such as ion doping, nanostructuring, surface coating, composite formation, and morphology control, directly influence key electrochemical properties, including capacity, rate capability and cycling stability. By systematically correlating each modification route with its impact on Na^+ storage behaviour and stability, this review offers novel insights for developing next-generation high-performance NTO-based anodes for SIBs.

2. Methodology

A comprehensive search of the literature was conducted using the following databases, sources, and networking platforms: Google Scholar, ResearchGate, and ScienceDirect (Elsevier) during the period of 8th of January 2024 to 30th of November 2025. The search was performed using the following keywords: ''Sodium ion battery'', ''Lithium ion battery'', ''anode'', ''Sodium titanates'', and ''Nanomaterial engineering''. Approximately 18 000 records were initially appeared. After filtering articles published between 2011 and 2025, about 7420 records remained. The most recent articles relevant to the subtopics addressed in the Results and Discussion section were selected for this review.

3. Recent progress on sodium titanates

Before providing a detailed discussion of the various modification strategies, it is important to first examine the fundamental properties and performance characteristics of commonly studied NTO materials. Accordingly, this section presents recent research progress on NTO-based anodes, including $NaTiO_2$, $Na_4Ti_5O_{12}$, $Na_2Ti_6O_{13}$, and $Na_2Ti_3O_7$.

3.1 $NaTiO_2$

O3-Type $NaTiO_2$ has been investigated as an anode material in SIB by Wu *et al.*,[20] who found that it could reversibly intercalate about 0.5 Na^+ per $NaTiO_2$, corresponding to a reversible capacity of 152 mAh g^{-1} at a C/10 rate. The material showed a capacity retention of over 98% after 60 cycles. They showed the reversible O3–O′3 phase transition of O3-$NaTiO_2$ upon sodiation and desodiation using *in situ* X-ray diffraction measurements. Vasileiadis and Wagemaker[21] predicted the kinetics and thermodynamics of the sodiation of hollandite TiO_2 theoretically *via* DFT calculations. Sodiation of TiO_2 up to the $NaTiO_2$ composition results in layered O3-type $NaTiO_2$, which can be used as a promising anode material for SIBs. They predicted that the stepwise sodiation of hollandite TiO_2 first yields $Na_{0.25}TiO_2$ and then O′3-$Na_{0.68}TiO_2$ at higher Na^+ concentrations. Further sodiation proceeds *via* a solid-solution formation mechanism towards the layered O3-$NaTiO_2$, potentially providing an alternative route to prepare this promising SIB anode that is otherwise challenging to synthesize. A two-step hydrothermal method was employed by Sun *et al.*[22] to synthesize hybrid NTO ($NaTi_8O_{13}/NaTiO_2$) nanoribbons directly grown on layered MXene Ti_3C_2. Owing to their unique structure and composition, the resulting NTO/Ti_3C_2 composite exhibited outstanding cycling stability and high-rate capability as a SIB anode, delivering a stable capacity of 82 mAh g^{-1} even after 1900 cycles at a current density of 2000 mA g^{-1}. $NaTiO_2$ nanotubes (NTO NTs) were grown *in situ* on $Ti_3C_2F_x$ to construct a hybrid anode for SIBs. The composite exhibited a high specific capacity of 130.2 mAh g^{-1} after 800 cycles at 100 mA g^{-1}, with nearly 100% coulombic efficiency. This superior performance arises from the perpendicular growth of NTO NTs on both sides of $Ti_3C_2F_x$, which enhances Na^+ diffusion and storage capacity.[23]

3.2 $Na_4Ti_5O_{12}$

Another type of NTO with the $Na_4Ti_5O_{12}$ stoichiometry has been investigated as a potential anode material for SIBs. The trigonal phase (T-$Na_4Ti_5O_{12}$) was reported by Woo *et al.*[24] and the monoclinic phase (M-$Na_4Ti_5O_{12}$) was reported by Naeyaert *et al.*[25]. Woo *et al.* showed that T-$Na_4Ti_5O_{12}$ exhibited a reversible intercalation/deintercalation of Na^+ ions, which delivered only 50 mAh g^{-1} specific capacity (12.8 mA g^{-1}). This study

mainly focused on using T-$Na_4Ti_5O_{12}$ as an anode material for LIBs, where intercalation/deintercalation of Li^+ ions resulted in a higher specific capacity of 100 mAh g^{-1} over 100 cycles. The poor specific capacity as a SIB anode is attributed to the poor kinetics of Na^+ ion intercalation/deintercalation due to steric hindrance from the larger Na^+ ion. On the other hand, Naeyaert *et al.* studied M-$Na_4Ti_5O_{12}$ and found a higher reversible capacity of 56 mAh g^{-1} (12.5 mA g^{-1}). M-$Na_4Ti_5O_{12}$ was expected to be more favourable for Na^+ ion intercalation/deintercalation, because M-$Na_4Ti_5O_{12}$ has a quasi-2D layered structure with partially filled Na sites, while T-$Na_4Ti_5O_{12}$ has a 3D framework with completely filled Na sites. Later, Tang *et al.*[26] fabricated monoclinic $Na_4Ti_5O_{12}$ nanoparticles embedded in porous carbon nanotubes. This unique porous hybrid structure improved the electrochemical performance of M-$Na_4Ti_5O_{12}$, with a capacity retention of 44.2 mAh g^{-1} after 3000 cycles at 1 A g^{-1}. Naeyaert *et al.*[27] successfully synthesized a monoclinic $Li_4Ti_5O_{12}$ (M-$Li_4Ti_5O_{12}$) phase analogous to $Na_4Ti_5O_{12}$, which exhibited good rate capability, with reversible capacities of 56 and 52 mAh g^{-1} at C/20 and 2C, respectively. They also developed an improved synthesis route for monoclinic $Na_4Ti_5O_{12}$ through M(III) ion doping (M = V, Cr, Mn, Fe, and Co). Doping enhanced the sodium stability of the monoclinic phase under ambient atmospheric conditions. However, the electrochemical performance of the doped phases was lower than that of undoped $Na_4Ti_5O_{12}$ in SIBs, likely due to structural alterations affecting the dimensions of the conduction pathways.

3.3 $Na_2Ti_3O_7$

The $Na_2Ti_3O_7$ structure has been mostly studied as a possible anode, with the lowest operating potential for SIBs. It can have a large interlayer spacing (up to about 8 Å), which may help with excellent cycling performance in SIBs, especially when high power is required.[28] Senguttuvan *et al.*[29] were the first to discover that $Na_2Ti_3O_7$ functions as an effective low-voltage insertion sodium compound because it can reversibly absorb 2 Na^+ ions per formula unit (200 mAh g^{-1}) with a low operating voltage plateau of 0.3 V *vs.* Na/Na^+. Subsequently, Pan *et al.*[30] found that the particle size of $Na_2Ti_3O_7$ has an impact on the sodium storage behavior and that the storage capacity of a nanosized $Na_2Ti_3O_7$ sample is higher than that of a microsized one. By optimizing the electrolyte and binder, it was found that the microsized $Na_2Ti_3O_7$ electrode delivers a reversible capacity of 188 mAh g^{-1} in 1 M NaFSI/PC electrolyte at 0.1C within 0.0–3.0 V voltage range, using sodium alginate as the binder. During the sodiation/desodiation process, Rudola *et al.*[31] detected an intermediate phase of $Na_{3-x}Ti_3O_7$. Based on *ex situ* XRD data, the two discharge plateaus observed during the sodiation process revealed the two-phase reactions $Na_2Ti_3O_7 \rightarrow Na_{3-x}Ti_3O_7$ and $Na_{3-x}Ti_3O_7 \rightarrow Na_4Ti_3O_7$. The Na storage pathway is lost in later cycles as a result of an irreversible transition brought on by the lower discharge plateau.

Yan *et al.*[32] reported a compound of $Na_2Ti_3O_7$ with a twine-like, three-dimensional network assembled with ultralong nanotubes. It had a superior rate capability of 80 mAh g^{-1}, maintained even at 50C, and 77% capacity retention after 1000 cycles at 10C. This enhanced performance was brought by its unique structure, which enhances the contact between material and electrolyte, reduces the Na^+/e^- transport path, and accommodates volume expansion during charging and discharging. Later, a new phase of $Na_2Ti_3O_7$ was synthesized by Cao *et al.*[33] for the first time, which belongs to the triclinic structure, in the $P\bar{1}$ space group. The synthesized triclinic $Na_2Ti_3O_7$ (t-NTO) had a shorter O–O band of the distorted TiO_6 octahedron and maintained a low charge potential plateau similar to that of the monoclinic $Na_2Ti_3O_7$ (m-NTO). This resulted in a more stable layered structure with minimal fluctuation and smoother Na^+ transport channels. According to *in situ* XRD, the m-NTO electrode undergoes an irreversible phase shift during the charge and discharge procedure, which significantly reduces the specific capacity. Nonetheless, the t-NTO electrode's structural evolution after sodiation is reversible, ensuring strong cycle stability. Pan *et al.*[34] assembled a layered-structured $Na_2Ti_3O_7$ electrode in full-cell battery configurations to evaluate its practical applicability. When tested in a coin cell, the electrode delivered a specific capacity of 77.2 mAh g^{-1} at 1 A g^{-1} after 10 000 cycles, with an outstanding capacity retention of 99.9%, indicating excellent cycling stability. In a soft-pack battery configuration, it exhibited specific capacities of 22.3 mAh g^{-1} at 0.1 A g^{-1} and 18.1 mAh g^{-1} at 0.05 A g^{-1} after 50 cycles. Moreover, post-cycling analysis revealed no evidence of sodium dendrite formation or active material shedding, confirming its high safety and structural integrity in practical applications.

3.4 $Na_2Ti_6O_{13}$

Trinh *et al.*[35] reported the reversible electrochemical activity of $Na_2Ti_6O_{13}$ in SIB. Later, Rudola *et al.*[36] elucidated the Na^+ insertion/extraction mechanism of $Na_2Ti_6O_{13}$ using *ex situ* XRD measurements. The mechanism is as follows: $Na_2Ti_6O_{13} + xNa^+ + xe^- \rightleftharpoons Na_{2+x}Ti_6O_{13}$ with $x = 0.85$. Cao *et al.*[37] synthesized $Na_2Ti_6O_{13}$ nanorods with large interlayer spacing, which provided facile channels for Na^+ insertion and extraction. This SIB anode, after activation, has an exceptional cycling stability of 109 mAh g^{-1} after 2800 cycles at 1 A g^{-1} and a high specific capacity of 172 mAh g^{-1} at 0.1 A g^{-1}. A green ball dianthus-like $Na_2Ti_6O_{13}$, with a tunnel structure and large interlayer space, was synthesized by Du *et al.*[19] The synthesized $Na_2Ti_6O_{13}$ showed good rate performance and outstanding cyclability as a SIB anode material. After 300 cycles, a high reversible capacity exceeding 100 mAh g^{-1} is delivered at 1000 mA g^{-1}. Despite 200 cycles at 500 mA g^{-1} and 200 cycles at 1000 mA g^{-1}, the electrode can sustainably support a capacity of 66 mAh g^{-1} at 2000 mA g^{-1} without exhibiting any discernible decay after 200 cycles. Wu *et al.*[38] investigated the origin of capacity fluctuation using a long-life $Na_2Ti_6O_{13}$ anode, which exhibited excellent cycling stability and superior rate performance. A maximum specific capacity of 160.7 mAh g^{-1} was achieved at the 80th cycle under a current density of 20 mA g^{-1}. However, the subsequent capacity decay was mainly attributed to the irreversible reduction reaction leading to the formation of

metallic titanium, structural reconstruction or relaxation of the electrode material, and increased electrode polarization during cycling. Later, S. Ghosh[39] used a sonochemical route to synthesize $Na_2Ti_6O_{13}$, which exhibited outstanding reversible electrochemical performance with up to 93% retention. Recently, Zhu *et al.*[40] synthesized $Na_2Ti_6O_{13}$ nanorods with a large interlayer spacing of approximately 0.798 nm and systematically studied the effect of calcination temperature on their electrochemical performance. The sample prepared at 800 °C exhibited the most favorable characteristics, delivering high discharge capacities of 168.2 mAh g^{-1} and 115.2 mAh g^{-1} at current densities of 20 mA g^{-1} and 500 mA g^{-1}, respectively, and maintaining 131.1 mAh g^{-1} and 96.7 mAh g^{-1} after 100 cycles. These results demonstrate that the nanorod morphology and enlarged interlayer spacing effectively enhance Na^+ diffusion, resulting in excellent cycling stability and rate performance.

3.5 $Na_2Ti_3O_7/Na_2Ti_6O_{13}$ hybrid structures

Several studies have reported hybrid structures of $Na_2Ti_6O_{13}$ and $Na_2Ti_3O_7$.[41–43] Cech *et al.*[41] synthesized and investigated single-phase $Na_2Ti_6O_{13}$ and mixed-phase $Na_2Ti_6O_{13}/Na_2Ti_3O_7$ titanates to evaluate their electrochemical performance. The mixed-phase electrode exhibited higher capacity and a broader active voltage range compared to the single-phase $Na_2Ti_6O_{13}$; however, it showed lower cycling stability. Specifically, $Na_2Ti_6O_{13}$ delivered an initial discharge capacity of 60 mAh g^{-1} at 0.1C, which was about half that of the mixed NTO (119 mAh g^{-1}). Cyclic voltammetry analyses revealed distinct electrochemical behaviours for each material: the sodium hexatitanate ($Na_2Ti_6O_{13}$) reaction was primarily diffusion-controlled, while the mixed-phase material containing $Na_2Ti_3O_7$ exhibited both diffusive and capacitive contributions to the overall electrode reaction. According to Wu *et al.*,[42] the reaction dynamics revealed that the sodium ion diffusion in tunnel $Na_2Ti_6O_{13}$ is faster than that of layered $Na_2Ti_3O_7$ (Fig. 1). Further, they found that the hybrid material combined the benefits of tunnel $Na_2Ti_6O_{13}$, which has high ionic conductivity and great cycling stability, with layered $Na_2Ti_3O_7$, which has a better capacity for storing Na. Because of the complementary qualities of the two distinct structures, there was an exceptional rate capability and cycling stability. Chandel *et al.*[43] fabricated a $Na_2Ti_6O_{13}/Na_2Ti_3O_7$ nanocomposite with an exceptional synergistic effect between the $Na_2Ti_6O_{13}$ and $Na_2Ti_3O_7$ phases that could effectively offset the disadvantages of individual phases.

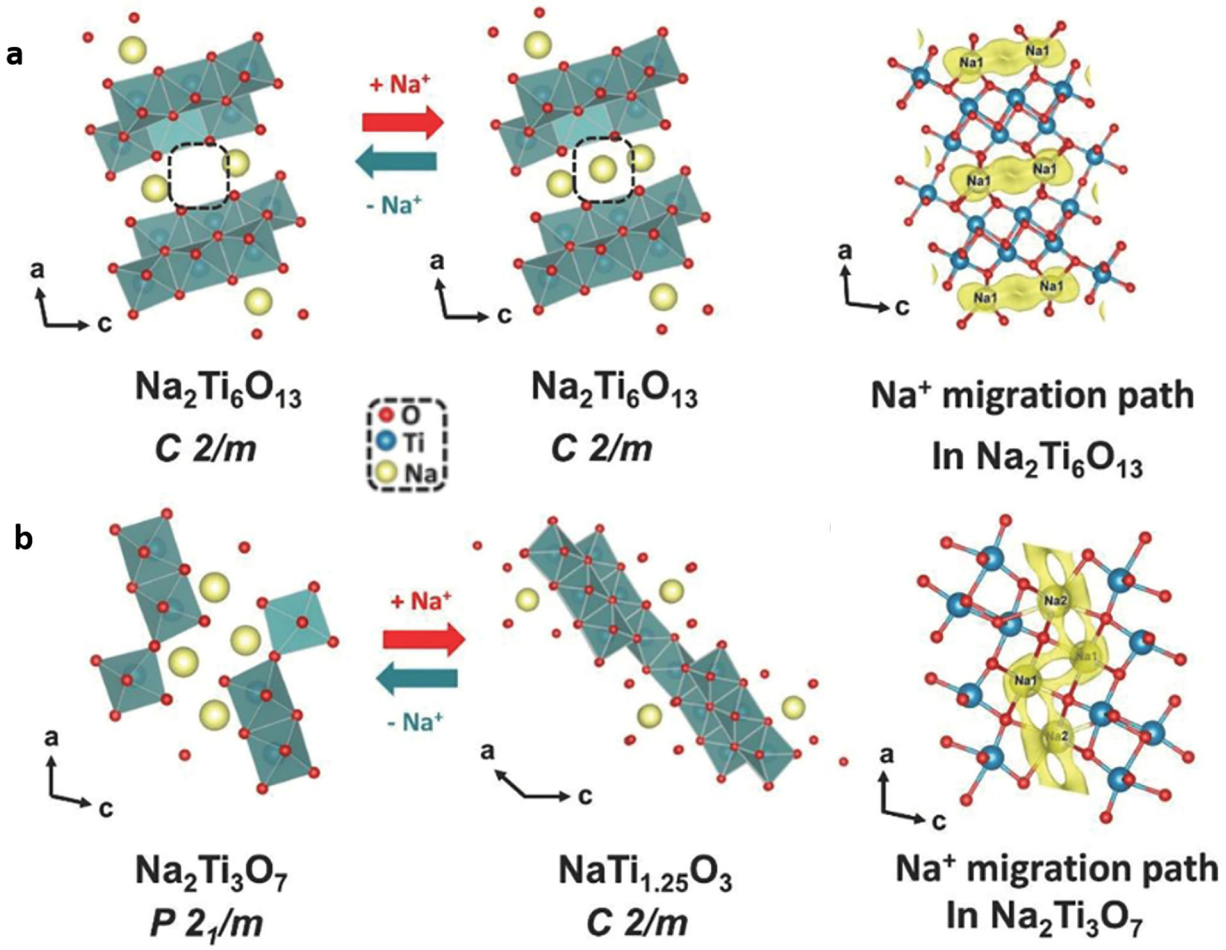

Fig. 1 Schematic representation and Na^+ migration paths in (a) tunnel $Na_2Ti_6O_{13}$ and (b) layered $Na_2Ti_3O_7$. Reproduced from ref. 42, licensed under Creative Commons Attribution License.

This was demonstrated by its superior cycling stability of 182 mAh g^{-1} at 100 mA g^{-1} after 165 cycles and high rate capability of 161 mAh g^{-1} at 500 mA g^{-1} over 100 cycles. Recently, Wang *et al.*[44] explored $Na_2Ti_3O_7$, $Na_2Ti_6O_{13}$, and mixed compositions, synthesized from titanium sources with different sulfur contents. It was found that a lower sulfur content level yielded single-phase $Na_2Ti_3O_7$. The mixed-phase material with higher $Na_2Ti_6O_{13}$ content demonstrated enhanced rate capability and cycling stability. Specifically, it delivered an initial discharge capacity of 57.4 mAh g^{-1} at 177 mA g^{-1} and retained 22.7 mAh g^{-1} after 1000 cycles, highlighting its potential as a potential NTO-based anode material.

4. Modification strategies to enhance the electrochemical performance of sodium titanates

Although NTO is a promising anode with a low voltage plateau, high chemical stability, low cost, minimum volume change, and eco-friendly features, its wide bandgap results in poor electronic conductivity, suppressing its electrochemical characteristics. Therefore, several strategies have been implemented to achieve a high electrochemical performance.[45] In this review, most widely used modification strategies, namely, nanostructure engineering,[46–49] ion doping,[50–53] carbon-based composites,[54–57] carbon coating,[58–60] and other surface modification techniques, such as surface coating with inert metal oxides, MXene-derived NTOs, and quantum-dot-based modifications,[61–63] are discussed.

4.1 Nanostructure engineering

The use of nano-engineered NTOs in SIB anodes has several advantages for enhanced electrochemical performance, as summarized in Table 1. Designing at the nanoscale can increase the surface area of the material and is beneficial for alleviating volume variation. Furthermore, nanosized structures can accelerate ion diffusion and charge transfer by reducing the ion and electron transportation distance. Therefore, nanomaterials such as nanofibers, nanotubes, nanowires, and nanoarrays have the potential to improve the electrochemical performance of SIB anodes.[64,65]

4.2 Ion doping

Ion doping can create lattice defects and modify the local crystal environment in the crystal lattice, which is an effective approach to improve electronic conductivity and electrochemical capacity. The creation of oxygen vacancies is a common outcome of certain doping techniques, which can enhance cycling stability and speed up Na^+ and electron kinetics. Further, the larger-ionic-radius-doped NTO materials can improve the specific capacity and rate capability of the anode materials by increasing the interlayer *d* spacing,[52,69–71] as depicted in Table 2.

4.3 Carbon-based composites

The use of carbon-based materials to make a composite is an effective way to improve the rate performance, cycling stability, and electronic conductivity of NTO anode materials (Table 3). For instance, reduced graphene oxide (rGO) is a widely studied option under carbon-based materials because of its high specific surface area and electronic conductivity. Further, rGO provides shorter diffusion paths and better wettability which allow faster movement of Na^+ ions. Also, it ensures proper contact between the electrode and the electrolyte. Therefore, hybridizing NTO along with carbon-based materials like rGO, has gained much attention in recent studies.[57,74,75]

4.4 Carbon coating

By applying a thin carbon coating on the NTO anode, the electrochemical performance of the SIB can be improved (Table 4). As the NTO materials have poor intrinsic electronic conductivity, application of a carbon coating can improve the electron conductivity and interfacial charge transfer of the anode. Moreover, depending on the study, carbon coating can provide channel pathways for improved ionic diffusion and inhibit crystal growth.[58,60]

4.5 Other surface modification techniques

Besides carbon coating, other methods to modify the surface of NTO anode materials have been developed. Surface coating by an inert metal oxide is one such method. Mukherjee *et al.*[61] synthesized surface-modified NTOs with carbon ($Na_2Ti_3O_7$@C) and zirconia ($Na_2Ti_3O_7$@ZrO_2) coatings. Both exhibited better electrochemical characteristics than $Na_2Ti_3O_7$ in their bare form because the thin covering layer helps prevent undesirable SEI development at the electrode–electrolyte interface. $Na_2Ti_3O_7$@C and $Na_2Ti_3O_7$@ZrO_2 had 75% and 68% capacity retention, respectively, after 100 cycles at 100 mA g^{-1}. Zhong *et al.*[81] successfully synthesized a pompon-like MXene-derived NTO ($Na_2Ti_3O_7$@C) with a carbon-encapsulated, cross-linked nanoribbon structure. The material features a suitable interlayer spacing and open porosity, facilitating ion diffusion and electrolyte infiltration. It demonstrated a high reversible capacity of 173 mAh g^{-1} at 200 mA g^{-1} and exhibited excellent cycling stability over 200 cycles, with only 0.026% capacity decay per cycle at 2 A g^{-1}. Surface modification of $Na_2Ti_3O_7$ nanofiber arrays was carried out with N-doped graphene quantum dots (N-GQDs) by Kong *et al.*[63] The distinct soft protection of the N-GQDs exhibited significantly enhanced surface conductivity, and the stability of the nanofibre array structure resulted in rapid Na^+ ion diffusion kinetics. This exhibited a capacity of 158 mAh g^{-1} after 30 cycles and retained ~92.5% of this capacity after 1000 cycles at 4C. According to Liu *et al.*,[62] surface-modulated single-crystalline $Na_2Ti_3O_7$ nanotube arrays with Ti^{3+} self-doping could deliver a high rate capability of 88.5 mAh g^{-1} at 100C and capacity retention of 92.32% at 50C after 5000 cycles. Yin *et al.*[82] developed Ag@$Na_2Ti_6O_{13}$ composites using silver as a novel conductive agent. Uniformly distributed nano-sized Ag particles (3%) enhanced the

Table 1 Summary of the nanostructured NTO anodes and their performance enhancements

Sample description	Synthesis process	Effect of the modification	Electrochemical enhancement	Ref.
Additive-free NTO nanotube array	Hydrothermal treatment	• The open structure of the NTO nanotube array offers more channels and shorter routes for the Na ions to diffuse easily, ensuring outstanding rate performance. • The structure integrates the benefits of both tunnel-type $Na_2Ti_6O_{13}$ and layered $Na_2Ti_3O_7$. • Good electrical contact between the array film and the Ti substrate enables high capacity retention.	• Rate performance of 42 mAh g^{-1} at a current density of 3200 mA g^{-1} • 55 mAh g^{-1} reversible capacity retains after 5000 cycles	64
$Na_2Ti_3O_7$ nanofibers	Electrospinning process and thermal treatment	• The 1D structure of the NTO results in improved electrochemical activity.	• Capacity of 257.8 mAh g^{-1} at 30 mA g^{-1} • Good rate capability	65
3D flower-like architecture consisting of 2D $Na_2Ti_3O_7$ nanosheets (Na-TNSs)	Hydrothermal process	• The open, nanoarchitectured structure offers abundant channels for Na^+ diffusion and improved electrolyte wettability. • 3D framework enhances electron/ion transport and maintains structural stability, resulting in high rate capability and long cycle life.	• 85 mAh g^{-1} discharge capacity after 1100 cycles with 80% capacity retention at 400 mA g^{-1} • At a high current density of at 800 mA g^{-1} capacity remained at 73.8 mAh g^{-1}	66
NTO@ reduced graphene oxide core–shell (NTO@GCS) nanowire aerogel	Hydrothermal method	• High flexibility, porosity, and conductivity. • The Na^+ kinetic diffusion is enhanced by the uniform 3–7 nm layer of rGO wrapped around the NTO nanowire, improving the long-term cycling stability.	• Reversible capacity of 240 mAh g^{-1} at 0.2C • Cycling stability with about 100% coulombic efficiency after 4900 cycles at 2C and 4C	47
PEDOT encapsulated NTO $[NaTi_3O_6(OH)\cdot 2H_2O]$ (PEDOT@NTO) nanowires	Hydrothermal method followed by *in situ* oxidative polymerization	• The coated PEDOT layers protect the structural stability of NTO throughout the charge/discharge processes and encourage ion diffusion and electron transport. • High specific capacity, along with excellent rate and cycling stabilities, is achieved due to the synergistic effects of the 3D architecture of intertwined nanowires and the multifunctional PEDOT shell.	• Capacity of 200.1 mAh g^{-1} at 20 mA g^{-1} • Capacity retention up to 76.4% after 1000 cycles at 200 mA g^{-1} • Reversible capacity of 80.5 mAh g^{-1} at a fairly high rate of 1000 mA g^{-1}	49
NTO ($Na_{1.4}H_{0.6}Ti_3O_7$) nanotubes	Hydrothermal method	• High surface area and nanoparticles contribute to the surface processes.	• Capacity retention of 92% after 170 cycles at 100 mA g^{-1} • Nearly 100% coulombic efficiency, even at low rates	48
Tunnel-type structured $Na_2Ti_6O_{13}$@C nanowires	—	• Optimal interlayer spacing and short diffusion paths enhance Na^+ kinetics and decrease activation energy at low temperatures.	• high reversible capacity of 100 mAh g^{-1} at 0 °C with 99.6% capacity retention after 200 cycles at 0.5C	67
1D single-crystal nanobelts (1D SCNs) and 1D SCN coupled carbon nanotubes (SCNs/CNTs)	—	• The 1D SCNs, with their large interlayer spacing, abundant active sites, strong mechanical stability, and efficient 1D self-assembly, exhibit favorable electrochemical kinetics and low-strain characteristics. • SCNs/CNTs film demonstrates excellent Na^+ storage performance, with high reversible capacity, fast charge/discharge rates, and long-term cycling stability.	• Long-term cycling stability of SCNs/CNTs delivering a reversible capacity of 163.6 mAh g^{-1} at 1C with 93% capacity retention and a high coulombic efficiency of about 100% over 1000 cycles (Fig. 2)	68

composite's conductivity, enabling excellent Na^+ insertion performance. The electrode delivered a discharge capacity of 189 mAh g^{-1} after 100 cycles with ~98% capacity retention. Mei *et al.*[83] proposed a combined oxygen-vacancy and bismuth-substitution strategy to transform intrinsically Na^+ sluggish $Na_2Ti_3O_7$ into a fast Na-ion conductor. The approach expands the interlayer spacing and generates *trans*-layer pathways, forming a 3D Na^+ transport network. Consequently, the modified material exhibited substantially improved reversible capacity, rate capability, and cycling stability, achieving ~145–210% performance enhancement compared with pristine NTO.

5. Outlook and practical perspectives

Despite the substantial progress achieved in recent years, several challenges must still be addressed before NTOs can

Table 2 Summary of the ion-doped NTO anodes

Sample description	Synthesis process	Effect of the modification	Electrochemical enhancement	Ref.
Sulfur-doped double-shell NTO ($Na_2Ti_3O_7$) microspheres	Hydrothermal synthesis with subsequent sulfurization	• S doping gives the sample additional Na^+ ion storage sites and improves its ionic conductivity, benefiting from increased cyclability and capacity. • Rapid ion movement and smooth electrolyte penetration are made possible by the double-shell structure.	• Specific capacity of 222 mAh g^{-1} at 1C • Cycling stability of 162 mAh g^{-1} after 15 000 cycles at 20C • Rate capability 122 mAh g^{-1} at 50C	50
Ti^{3+} self-doped $Na_2Ti_3O_7$	Sol–gel process followed by post-heat treatment	• Exhibits enhanced electron conductivity and ion diffusion capabilities due to self-doped Ti^{3+} with a larger ionic radius and greater electronic conductivity.	• Specific capacity of 187.8 and 51.9 mAh g^{-1} from 0.1C to 10C	53
Zirconium-doped hydrogenated $Na_2Ti_3O_7$ (HNTOZr)	Hydrothermal process followed by hydrogenation	• The larger size Zr-doped NTO results in an increase in interlayer spacing, which contributes to an improvement in specific capacity.	• Discharge capacity of ~200 mAh g^{-1} at 200 mA g^{-1} • Cycling stability up to 2500 cycles with 99.70% coulombic efficiency	69
Molybdenum-doped NTO	Solvothermal method	• Incorporating Mo^{6+} into the NTO crystal structure creates oxygen vacancies, and Ti^{4+} is partially reduced to Ti^{3+}. This facilitates faster Na^+ ion storage kinetics and greatly increases electrical conductivity *via* several techniques.	• Specific capacity of ~152.9 mAh g^{-1} at of 1 A g^{-1} • Cycling stability up to 2500 cycles with 100% coulombic efficiency	70
Vanadium-doped sodium titanate	Sol–gel method	• V^{5+} doping leads to the transformation of the major phase of $Na_2Ti_3O_7$ to a single $Na_2Ti_6O_{13}$ phase at optimized doping concentrations. • Doping partially converts Ti^{4+} to Ti^{3+}, which has an additional electron to improve the electronic conductivity and creates oxygen vacancies to preserve charge neutrality and facilitate electron and ion transport. • Oxygen vacancies further maintain the electrode's integrity, which results in long-term cycling.	• Capacity of 136 mAh g^{-1} at 100 mA g^{-1} after 900 cycles • Rate capacity of 101 mAh g^{-1} at 1000 mA g^{-1}	71
Selenium-doped $Na_2Ti_3O_7$ array ($Na_2Ti_3O_6Se$)	—	• Se doping increases reaction kinetics by greatly enlarging the interlayer spacing, narrowing the bandgap, and lowering the Na^+ diffusion barrier.	• Reversible capacity of 207 mAh g^{-1} after 100 cycles at 0.2 A g^{-1} • Capacity of 155 mAh g^{-1} after 1000 cycles at 1 A g^{-1}	52
Copper-doped $Na_2Ti_3O_7$	Hydrothermal method	• Cu-doped $Na_2Ti_3O_7$ exhibits 2.5 times higher electronic conductivity and a 9.5% larger unit cell volume than non-doped NTO due to a ~1 eV reduction in band gap and structural evolution.	• 85% capacity retention over 300 cycles at 2C	72
Potassium-doped $Na_2Ti_3O_7$	Microwave heating method	• The doping of K^+ through partial substitution of Na^+ in NTO enhances performance, primarily due to the increased exposure of the Na^+ storage (100) plane, expanded interlayer spacing, and stabilized layered structure.	• Reversible specific capacity of 162 mAh g^{-1} at 0.1C • Capacity retention of 75% after 8200 cycles at 1C or 4000 cycles at 10C	73

Table 3 Summary of the NTO/carbon-based composite anode materials and their performance enhancements

Sample description	Synthesis process	Effect of the modification	Electrochemical enhancement	Ref.
Sodium titanate-carbon ($Na_2Ti_3O_7$/C) composite	Rheological phase method	• When carbon and $Na_2Ti_3O_7$ are tightly integrated, the electrical conductivity increases, the charge transfer resistance decreases, and the electrochemical stability improves during cycling.	• Discharge capacity of 72.8 mAh g^{-1} after 100 cycles at a rate of 5C • Discharge capacity of 111.8 mAh g^{-1} at 1C after 100 cycles	74
$Na_2Ti_3O_7$ nanowires embedded into (3D) rGO	Solvothermal synthesis	• rGO can permit substantial Na^+ ion insertion as an active host and provide a high reversible capacity over a long cycle life at high current densities. • Therefore, the close integration of rGO and $Na_2Ti_3O_7$ provides high surface area, mitigates volume expansion, reduces charge transfer resistance, and enhances cyclic stability.	• Reversible capacity of ~134 mAh g^{-1} after 300 cycles at 100 mA g^{-1} • Rate capacity of 116 mAh g^{-1} even at 2000 mA g^{-1}	54
Sandwich-structured $Na_2Ti_3O_7$ nanowires@ carbon nanotubes (NTONW@CNT) and graphene oxide	Hydrothermal-assisted modified vacuum filtration	• Added CNTs improve the conductivity of the nanowires by connecting them and facilitating the uniform dispersion of the nanowires and nanotubes. • Many electron-transfer channels are provided by this sandwich-like layered-structured film, which enhances reaction kinetics throughout the charging and discharging process.	• Reversible capacity of 92.5 mAh g^{-1} after 100 cycles at 2C • Discharge capacity of 59.9 mAh g^{-1} at 5C after 100 cycles	55
Encapsulated hollow $Na_2Ti_3O_7$ spheres in rGO films	Hydrothermal method followed by vacuum-assisted filtration	• The voids between the carbon sheets and the hollow structure allow for the accommodation of strain and volume expansion during charging and discharging • The transportation of electrons and ions is optimized *via* thin NTO nanosheet interactions with the rGO sheets, enhancing the rate performance.	• Reversible capacity of 222 mAh g^{-1} after 200 cycles at 50 mA g^{-1} • Rate performance of 135 mAh g^{-1} at 500 mA g^{-1}	56
Dense sandwich-like $Na_2Ti_3O_7$@rGO composite	Hydrothermal route	• rGO in the composite maintains high surface area. • The structure reduces the spacing between NTO nanoparticles, which will shorten the Na^+ ion diffusion channel and speed up migration.	• Reversible capacity of 137 mAh g^{-1} at 100 mA g^{-1} after 500 cycles • Rate performance of 92 mAh g^{-1} at 2000 mA g^{-1}	75
rGO integrated $Na_2Ti_6O_{13}$ nanocomposite	Solvothermal method	• rGO-$Na_2Ti_6O_{13}$ integration creates a large surface area for the electrode–electrolyte interaction, lowers charge transfer resistance, boosts electrical conductivity, and acts as a buffer to lessen volume expansion and contraction during Na^+ ion (de)insertion.	• High capacity ranging from ~214 to ~162 mAh g^{-1} at current densities in the range of 100–2000 mA g^{-1}, along with long cycling life	57
Sandwich-structured $Na_2Ti_6O_{13}$/rGO composite	Liquid-phase exfoliation and restacking method	• Exhibits significant enhancements in reversible discharge capacity and cycling stability.	• Discharge capacity of 196.5 mAh g^{-1} at a current density of 0.1 A g^{-1} after 500 cycles	76

be widely implemented as practical anode materials for SIBs. NTOs offer compelling advantages, including low operating potential, excellent structural stability, high safety, minimal volume change, and environmental friendliness, which make them particularly attractive for large-scale and stationary energy storage applications. In addition, their compatibility with diverse modification strategies, such as nanostructuring, ion doping, carbon coating, compositing, and surface engineering, provides multiple pathways to minimize their intrinsic limitations. However, the inherently low electronic conductivity, sluggish Na^+ ion diffusion kinetics compared to hard carbon, and the complexity of synthesis routes for some of the nanostructured or hybrid NTO systems remain notable challenges.

Nanostructure engineering of NTO material can boost rate performance due to the shortened ion/electron paths, enhanced surface area, and 3D Na^+ diffusion channels. The

Table 4 Summary of the C-coated NTOs

Sample description	Synthesis process	Effect of the modification	Electrochemical enhancement	Ref.
Carbon-coated $Na_2Ti_3O_7$ nanotubes (NTs)	Solvothermal method	• During cycling, the outer layer of carbon strengthens the stability of the $Na_2Ti_3O_7$ NTs structure and increases its electron conductivity. • NTs combined with carbon layers allow for quick Na^+ diffusion and transport, ensuring favourable transport kinetics.	• Reversible capacity of 142.2 mAh g^{-1} for over 100 cycles at 1C • Rate capability of 83.75 mAh g^{-1} at 10C	77
$Na_2Ti_3O_7$@N-doped carbon hollow spheres	Stober method followed by hydrothermal treatment	• $Na_2Ti_3O_7$ hollow spheres deliver excellent Na storage performance, attributed to their unique ultrathin nanosheet-assembled structure that shortens ion diffusion paths and the N-doped carbon coating that enhances electronic conductivity.	• Rate performance, maintaining over 60 mAh g^{-1} after 1000 cycles at 50C	78
Carbon-coated layered $Na_2Ti_3O_7$ and tunnel $Na_2Ti_6O_{13}$ hybrid	Using supercritical methanol followed by heat treatment	• C coated on the hybrid caused a phase transition from $Na_2Ti_3O_7$ to $Na_2Ti_6O_{13}$ • As some Na^+ ions can be inserted/removed from the layered $Na_2Ti_3O_7$, the hybrid demonstrates a high rate performance and cycling stability. • The presence of $Na_2Ti_6O_{13}$ preserves the structural integrity of the entire hybrid.	• Capacity of 44 mAh g^{-1} at 1 A g^{-1}	79
Hydrogenated and carbon-coated $Na_2Ti_2O_5$ (H-$Na_2Ti_2O_5$@C)	hydrothermal method and synchronous hydrogenation and carbonization	• Hydrogenation leads to partially reduced titanium • Coating layer enhances electron transport and suppresses volume expansion, stabilizing the $Na_2Ti_6O_{13}$ anode and greatly improving its cycling stability.	• Enhanced rate capability with a capacity of 165 mAh g^{-1} at 8C	80
Carbon-coated $Na_2Ti_3O_7$	Solid-state synthesis	• Special cuboid-shaped microstructure and C coating cause a synergistic effect that lowers the resistance due to surface film and high Na^+ ion diffusivity.	• Reversible capacities of 239, 168, 113, 102 and 70 mAh g^{-1} at 0.1, 0.2, 0.5, 1.0 and 2.0C rates	59
Carbon-coated $Na_2Ti_6O_{13}$	Post-heat-treatment process	• C-coated NTO increases electrical conductivity, reduces the impurity phase, and creates self-doping with Ti^{3+}, improving cyclic stability.	• Capacity of 150 mAh g^{-1} after 100 cycles at a current density of 50 mA g^{-1} • Capacity of 106 mAh g^{-1} at 800 mA g^{-1} even after 1000 cycles (Fig. 3a and b)	58
Carbon-coated $Na_2Ti_3O_7$	*In situ* and *ex situ* methods	• C coating enhances the electrical conductivity of the active material and regulates the production of SEI resulting from electrolyte deterioration.	• Rate performance of ~67 mAh g^{-1} at 1.5 A g^{-1} and a capacity retention of ~74.75% after 100 cycles (by *ex situ* method) • Reversible capacity of 52 mAh g^{-1} at 100 mA g^{-1} (by *in situ* method) (Fig. 3c)	60

disadvantages of nanostructure engineering involve potential pseudocapacitive loss and synthesis complexity. Potential loss of pseudocapacitive behaviour in NTO nanoforms arises when nanostructure engineering over-emphasizes bulk diffusion-controlled intercalation over surface-driven pseudocapacitance, reducing fast charge-storage contributions. Carbon coatings or composites improve conductivity, stabilize SEI, and improve cycle life, mainly by reducing charge-transfer resistance. However, there can be reductions in gravimetric capacity due to the added weight. Ion doping lowers the band gap and activation energy, and boosts diffusion coefficients, resulting in improved conductivities and rate capabilities. However, it is possible to have a slight capacity drop and a potential rise.

From a practical perspective, achieving a balance between performance enhancement, material cost, scalable synthesis, and electrode processing remains a critical challenge. While it is unlikely that NTOs will completely replace hard carbon as the universal ''gold-standard'' anode for all SIB applications in the near future, their notable cycling stability, safety characteristics, and low-voltage operation position them as highly promising candidates for specific applications, particularly in long-life, high-power, and stationary storage systems. Continued efforts toward scalable synthesis, conductivity enhancement, and full-cell optimization are therefore essential to unlock the full practical potential of NTO-based anodes in next-generation SIBs.

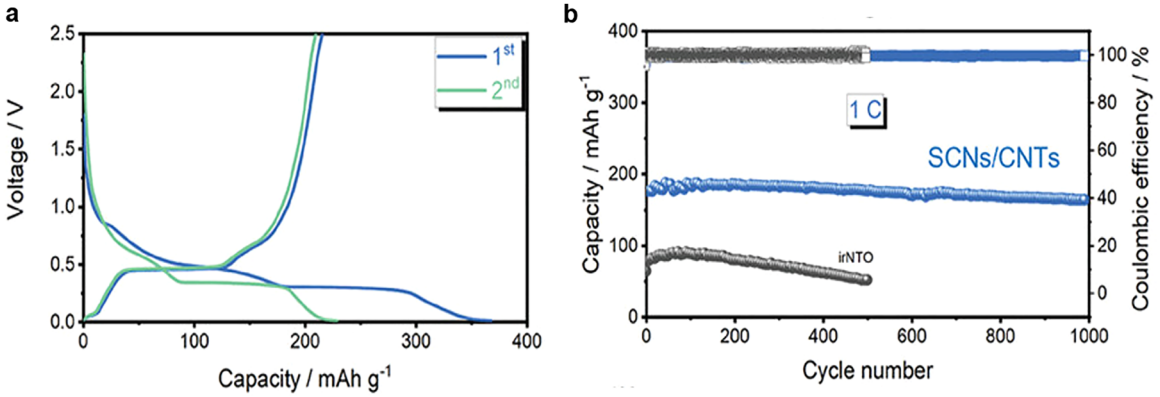

Fig. 2 (a) Typical charge/discharge profiles at 0.1C. (b) Cycling performance at 1C. Reproduced from ref. 68, licensed under Creative Commons Attribution-NonCommercial-NoDerivs Licence.

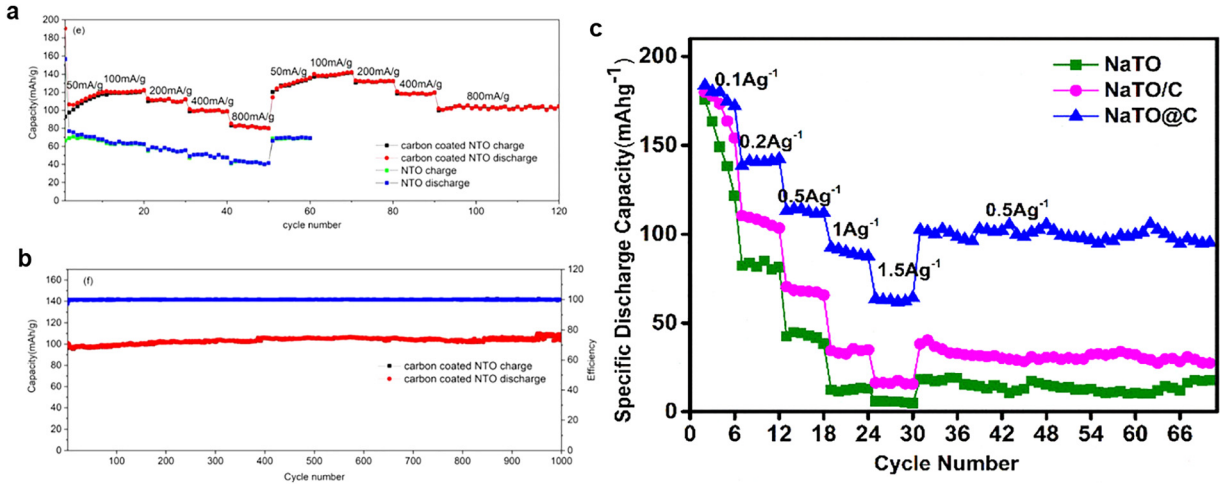

Fig. 3 (a) Rate performance of carbon-coated NTO, (b) capacity retention for carbon-coated NTO at charge/discharge rates of 800 mA g^{-1}. Reproduced from ref. 58, licenced under Creative Commons Attribution 4.0 License; and (c) rate performance of bare $Na_2Ti_3O_7$ (NaTO), *in situ* NaTO/C, and *ex situ* NaTO@C at different current densities. Reproduced from ref. 60, licenced under Creative Commons Attribution-NonCommercial-NoDerivs Licence.

6. Conclusions

NTO is a promising SIB anode material with a low voltage plateau of 0.3 V *vs.* Na/Na^+ for $Na_2Ti_3O_7$. Further, layered $Na_2Ti_3O_7$ can intercalate 2 Na^+ ions per formula unit. Besides layered $Na_2Ti_3O_7$, tunnel $Na_2Ti_6O_{13}$ is a widely used anode that can diffuse Na^+ faster. Hybrid compounds made with $Na_2Ti_3O_7$ and $Na_2Ti_6O_{13}$ have high ionic conductivity and great cycling stability due to the synergetic effects of both types of NTOs. However, individual NTOs have relatively poor electrochemical characteristics due to their wide bandgaps, which results in low electronic conductivity. Therefore, as a means to enhance the electrochemical performance of NTOs, several modification strategies including nanostructure engineering, ion doping, carbon-based composite synthesis, and surface modification strategies such as carbon coating have been developed.

Nanostructure engineering is beneficial for NTO anodes because the nanomaterials have a large surface area and accelerate ion diffusion and charge transfer by reducing the ion and charge transfer distances. This contributes to the increased Na^+ kinetics and improves long-term cycling stability. Ion doping has the potential to promote mechanisms such as creating oxygen vacancies or enlarging the interlayer *d* spacing. In most cases, doping can partially convert Ti^{4+} to Ti^{3+}, generating an additional electron to improve the electronic conductivity. Nanocomposites made with carbon-based materials can take advantage of both the NTO nanostructures and carbon-based materials to function as an effective high-performance anode material with high electronic conductivities and robust rate capacities. A thin layer of carbon coated on the surface of the NTO can significantly increase the conductivity of the anode material. Surface modification can also be carried out by introducing inert metal oxide layers to increase the cycling stability and rate performance of NTO anode materials. In general, the performance of anode materials for SIBs can be enhanced with these modification techniques, as evidenced by

the literature reported studies which are summarized in this review.

In the quest for feasible SIBs, there are undoubtedly still many difficult obstacles to overcome before large-scale energy storage systems can employ sodium as a charge carrier. Nevertheless, NTOs as anode materials merit additional research. Moreover, to improve the usage of SIBs in energy storage applications, more thorough research on the modification of anode materials needs to be actively pursued.

Author contributions

W. P. U. S. Wickramarathna: conceptualization, investigation, data curation, formal analysis, visualization, writing – original draft. N. P. W. Rathuwadu: conceptualization, investigation, formal analysis, writing – review and editing, resources, supervision, project administration, funding acquisition.

Conflicts of interest

There are no conflicts to declare.

Data availability

No new data were created or analysed in this review. All data discussed are from previously published studies and are cited in the reference list.

Acknowledgements

The authors gratefully acknowledge General Sir John Kotelawala Defence University Research Grants for the financial assistance under grant no. KDU/RG/2023/CARE/001.

Notes and references

1 A. K. Thakur, M. S. Ahmed, G. Oh, H. Kang, Y. Jeong and R. Prabakaran, *et al.*, Advancement in graphene-based nanocomposites as high capacity anode materials for sodium-ion batteries, *J. Mater. Chem. A*, 2021, **9**(5), 2628–2661.

2 K. C. Wasalathilake, H. Li, L. Xu and C. Yan, Recent advances in graphene based materials as anode materials in sodium-ion batteries, *J. Energy Chem.*, 2020, **42**, 91–107.

3 T. Kim, W. Song, D. Y. Son, L. K. Ono and Y. Qi, Lithium-ion batteries: outlook on present, future, and hybridized technologies, *J. Mater. Chem. A*, 2019, **7**(7), 2942–2964.

4 C. M. Costa, J. C. Barbosa, R. Gonçalves, H. Castro, F. J. D. Campo and S. Lanceros-Méndez, Recycling and environmental issues of lithium-ion batteries: Advances, challenges and opportunities, *Energy Storage Mater.*, 2021, **37**, 433–465.

5 S. Guo, J. Yi, Y. Sun and H. Zhou, Recent advances in titanium-based electrode materials for stationary sodium-ion batteries, *Energy Environ. Sci.*, 2016, **9**(10), 2978–3006.

6 W. Zhang, F. Zhang, F. Ming and H. N. Alshareef, Sodium-ion battery anodes: Status and future trends, *EnergyChem*, 2019, **1**(2), 100012.

7 Y. Xu, Y. Zhu, Y. Liu and C. Wang, Electrochemical performance of porous carbon/tin composite anodes for sodium-ion and lithium-ion batteries, *Adv. Energy Mater.*, 2013, **3**(1), 128–133.

8 J. Y. Hwang, S. T. Myung and Y. K. Sun, Sodium-ion batteries: Present and future, *Chem. Soc. Rev.*, 2017, **46**(12), 3529–3614.

9 J. Libich, J. Minda, M. Sedlaříková, J. Vondrák, J. Máca and M. Fíbek, *et al.*, Sodium-ion batteries: Electrochemical properties of sodium titanate as negative electrode, *J. Energy Storage*, 2020, **27**, 101150.

10 A. Siebert, X. Dou, R. Garcia-diez, D. Buchholz, F. Roberto and E. Handick, *et al.*, Solid Electrolyte Interphase Formation on Anatase TiO_2 Nanoparticle-Based Electrodes for Sodium-Ion Batteries, *ACS Appl. Energy Mater.*, 2024, **7**(1), 125–132.

11 Y. Yan, Y. X. Yin, Y. G. Guo and L. J. Wan, A sandwich-like hierarchically porous carbon/graphene composite as a high-performance anode material for sodium-ion batteries, *Adv. Energy Mater.*, 2014, **4**(8), 2–6.

12 J. Ding, H. Wang, Z. Li, A. Kohandehghan, K. Cui and Z. Xu, *et al.*, Carbon nanosheet frameworks derived from peat moss as high performance sodium ion battery anodes, *ACS Nano*, 2013, **7**(12), 11004–11015.

13 H. Xie, W. P. Kalisvaart, B. C. Olsen, E. J. Luber, D. Mitlin and J. M. Buriak, Sn-Bi-Sb alloys as anode materials for sodium ion batteries, *J. Mater. Chem. A*, 2017, **5**(20), 9661–9670.

14 M. Hu, Y. Jiang, W. Sun, H. Wang, C. Jin and M. Yan, Reversible conversion-alloying of Sb_2O_3 as a high-capacity, high-rate, and durable anode for sodium ion batteries, *ACS Appl. Mater. Interfaces*, 2014, **6**(21), 19449–19455.

15 F. Zhang, J. Zhu, D. Zhang, U. Schwingenschlögl and H. N. Alshareef, Two-Dimensional SnO Anodes with a Tunable Number of Atomic Layers for Sodium Ion Batteries, *Nano Lett.*, 2017, **17**(2), 1302–1311.

16 Y. C. Lu, C. Ma, J. Alvarado, T. Kidera, N. Dimov and Y. S. Meng, *et al.*, Electrochemical properties of tin oxide anodes for sodium-ion batteries, *J. Power Sources*, 2015, **284**, 287–295.

17 D. Su, X. Xie and G. Wang, Hierarchical mesoporous sno microspheres as high capacity anode materials for sodium-ion batteries, *Chem. – Eur. J.*, 2014, **20**(11), 3192–3197.

18 S. Tan, H. Yang, Z. Zhang, X. Xu, Y. Xu and J. Zhou, *et al.*, The Progress of Hard Carbon as an Anode Material in Sodium-Ion Batteries, *Molecules*, 2023, **28**(7), 3134.

19 X. Du, H. Yao, M. Ma, T. Feng, B. Zhang and Y. Xu, *et al.*, Green ball dianthus-like $Na_2Ti_6O_{13}$ as high-rate performance anode for sodium-ion batteries, *J. Alloys Compd.*, 2017, **721**, 100–105.

20 D. Wu, X. Li, B. Xu, N. Twu, L. Liu and G. Ceder, $NaTiO_2$: a layered anode material for sodium-ion batteries, *Energy Environ. Sci.*, 2015, **8**(1), 195–202.

21 A. Vasileiadis and M. Wagemaker, Thermodynamics and Kinetics of Na-Ion Insertion into Hollandite-TiO_2 and O3-Layered $NaTiO_2$: An Unexpected Link between Two Promising Anode Materials for Na-Ion Batteries, *Chem. Mater.*, 2017, **29**(3), 1076–1088.

22 X. Sun, K. Tan, Y. Liu, J. Zhang, L. Hou and C. Yuan, In situ growth of hybrid $NaTi_8O_{13}$/$NaTiO_2$ nanoribbons on layered MXene Ti_3C_2 as a competitive anode for high-performance sodium-ion batteries. Chinese, *Chem. Lett.*, 2020, **31**(9), 2254–2258.

23 K. Ming, Z. Zhang and L. Haibo, In situ growth of $NaTiO_2$ nanotubes on $Ti_3C_2F_x$ for enhanced sodium ion batteries, *Mater. Lett.*, 2022, **309**, 131457.

24 S. H. Woo, Y. Park, W. Y. Choi, N.-S. Choi, S. Nam and B. Park, *et al.*, Trigonal $Na_4Ti_5O_{12}$ Phase as an Intercalation Host for Rechargeable Batteries, *J. Electrochem. Soc.*, 2012, **159**(12), A2016–A2023.

25 P. J. P. Naeyaert, M. Avdeev, N. Sharma, H. B. Yahia and C. D. Ling, Synthetic, structural, and electrochemical study of monoclinic $Na_4Ti_5O_{12}$ as a sodium-ion battery anode material, *Chem. Mater.*, 2014, **26**(24), 7067–7072.

26 Y. Tang, L. Liu, Y. Zhang, H. Zhao, L. Kong and S. Gao, Confined formation of monoclinic $Na_4Ti_5O_{12}$ nanoparticles embedded into porous CNTs: towards enhanced electrochemical performances for sodium ion batteries, *New J. Chem.*, 2018, **42**(24), 19340–19343.

27 P. J. P. Naeyaert, M. Avdeev and C. D. Ling, Synthesis, electrochemistry and transition metal-doping of monoclinic $Li_4Ti_5O_{12}$ and $Na_4Ti_5O_{12}$, *Solid State Ionics.*, 2020, **353**, 115375.

28 Y. Xu, D. Bauer, M. Lübke, T. E. Ashton, Y. Zong and J. A. Darr, High-power sodium titanate anodes; a comparison of lithium vs sodium-ion batteries, *J. Power Sources*, 2018, **408**, 28–37.

29 P. Senguttuvan, G. Rousse, V. Seznec, J. Tarascon and M. R. Palacin, ChemInform Abstract: $Na_2Ti_3O_7$: Lowest Voltage Ever Reported Oxide Insertion Electrode for Sodium Ion Batteries, *ChemInform*, 2011, **42**(49), 4109–4111.

30 H. Pan, X. Lu, X. Yu, Y. S. Hu, H. Li and X. Q. Yang, *et al.*, Sodium storage and transport properties in layered $Na_2Ti_3O_7$ for room-temperature sodium-ion batteries, *Adv. Energy Mater.*, 2013, **3**(9), 1186–1194.

31 A. Rudola, N. Sharma and P. Balaya, Introducing a 0.2 V sodium-ion battery anode: the $Na_2Ti_3O_7$ to $Na_{3-x}Ti_3O_7$ pathway, *Electrochem. Commun.*, 2015, **61**, 10–13.

32 X. Yan, D. Sun, J. Jiang, W. Yan and Y. Jin, Self-assembled twine-like $Na_2Ti_3O_7$nanostructure as advanced anode for sodium-ion batteries, *J. Alloys Compd.*, 2017, **697**, 208–214.

33 Y. Cao, Q. Ye, F. Wang, X. Fan, L. Hu and F. Wang, *et al.*, A New Triclinic Phase $Na_2Ti_3O_7$ Anode for Sodium-Ion Battery, *Adv. Funct. Mater.*, 2020, **30**(39), 1–9.

34 J. Pan, N. Wang, D. Lv, W. Dong, J. Yang and F. Huang, Layered Structure $Na_2Ti_3O_7$ as a Promising Anode Material for Sodium-Ion Batteries, *Adv. Energy Sustainable Res.*, 2021, **2**(6), 2000095.

35 N. D. Trinh, O. Crosnier, S. Schougaard and T. Brousse, Synthesis, Characterizations and Electrochemical Studies of $Na_2Ti_6O_{13}$ for Sodium Ion Batteries, *ECS Meet Abstr.*, 2012, **MA2012–02**(15), 1851.

36 A. Rudola, K. Saravanan, S. Devaraj, H. Gong and P. Balaya, $Na_2Ti_6O_{13}$: a potential anode for grid-storage sodium-ion batteries, *Chem. Commun.*, 2013, **49**(67), 7451–7453.

37 K. Cao, L. Jiao, W. K. Pang, H. Liu, T. Zhou and Z. Guo, *et al.*, $Na_2Ti_6O_{13}$ Nanorods with Dominant Large Interlayer Spacing Exposed Facet for High-Performance Na-Ion Batteries, *Small*, 2016, **12**(22), 2991–2997.

38 C. Wu, Z. Wu, X. Zhang, R. Rajagopalan, B. Zhong and W. Xiang, *et al.*, Insight into the Origin of Capacity Fluctuation of $Na_2Ti_6O_{13}$ Anode in Sodium Ion Batteries, *Appl. Mater Interphases*, 2017, **9**(50), 43596–43602.

39 S. Ghosh, Sonochemically synthesized $Na_2Ti_6O_{13}$ nanorod: an efficient electrode material for Na-ion battery, *Bull. Mater. Sci.*, 2020, **43**(1), 251.

40 L. Zhu, X. Yin, C. Pan, Q. Han, Y. Miao and J. Liu, *et al.*, Facile synthesis of nanorods $Na_2Ti_6O_{13}$ as anode materials for high-performance sodium ion batteries, *J. Alloys Compd*, 2022, **906**, 164306.

41 O. Cech, K. Castkova, L. Chladil, P. Dohnal, P. Cudek and J. Libich, *et al.*, Synthesis and characterization of $Na_2Ti_6O_{13}$ and $Na_2Ti_6O_{13}$/$Na_2Ti_3O_7$ sodium titanates with nanorod-like structure as negative electrode materials for sodium-ion batteries, *J. Energy Storage*, 2017, **14**, 391–398.

42 C. Wu, W. Hua, Z. Zhang, B. Zhong, Z. Yang and G. Feng, *et al.*, Design and Synthesis of Layered $Na_2Ti_3O_7$ and Tunnel $Na_2Ti_6O_{13}$ Hybrid Structures with Enhanced Electrochemical Behavior for Sodium-Ion Batteries, *Adv. Sci.*, 2018, **5**(9), 1800519.

43 S. Chandel, S. Lee, S. Lee, S. Kim, S. P. Singh and J. Kim, *et al.*, Hierarchically nanorod structured $Na_2Ti_6O_{13}$/$Na_2Ti_3O_7$ nanocomposite as a superior anode for high-performance sodium ion battery, *J. Electroanal. Chem.*, 2020, **877**, 114747.

44 Z. Wang, R. Zhang, L. Chen, L. Cao, X. Guo and Z. Wu, *et al.*, Design of $Na_2Ti_3O_7$/$Na_2Ti_6O_{13}$ nanorods for sodium-ion batteries from titanium oxysulfate solution, *J. Electroanal. Chem.*, 2024, **972**, 118621.

45 Z. Liu, X. Zhang, D. Huang, B. Gao, C. Ni and L. Wang, *et al.*, Confined seeds derived sodium titanate/graphene composite with synergistic storage ability toward high performance sodium ion capacitors, *Chem. Eng. J.*, 2020, **379**, 122418.

46 L. Que, F. Yu, L. Zheng, Z. B. Wang and D. Gu, Tuning lattice spacing in titanate nanowire arrays for enhanced sodium storage and long-term stability, *Nano Energy*, 2018, **45**, 337–345.

47 N. Q. Tran, T. A. Le and H. Lee, An ultralight and flexible sodium titanate nanowire aerogel with superior sodium storage, *J. Mater. Chem. A*, 2018, **6**(36), 17495–17502.

48 M. M. Leite, V. L. Martins, F. M. Vichi and R. M. Torresi, Electrochemistry of sodium titanate nanotubes as a negative electrode for sodium-ion batteries, *Electrochim. Acta*, 2020, **331**, 135422.

49 Q. Zhang, Y. He, P. Mei, X. Cui, Y. Yang and Z. Lin, Multifunctional PEDOT-engineered sodium titanate nanowires

for sodium-ion batteries with synchronous improvements in rate capability and structural stability, *J. Mater. Chem. A*, 2019, **7**(33), 19241–19247.

50 N. Wang, X. Xu, T. Liao, Y. Du, Z. Bai and S. Dou, Boosting Sodium Storage of Double-Shell Sodium Titanate Microspheres Constructed from 2D Ultrathin Nanosheets via Sulfur Doping, *Adv. Mater.*, 2018, **30**(49), 1804157.

51 S. Pérez-Villar, E. Castillo-Martínez, J. M. López del Amo, T. Rojo and M. Armand, Electrochemical performance of novel O3 layered Al,Mg doped titanates as anode materials for Na-ion batteries, *Mater. Res. Bull.*, 2017, **94**, 199–207.

52 L. Gao, Y. Ma and M. Cao, Self-supported Se-doped $Na_2Ti_3O_7$ arrays for high performance sodium ion batteries, *Int. J. Hydrogen Energy*, 2024, **49**, 1–10.

53 T. Song, S. Ye, H. Liu and Y. G. Wang, Self-doping of Ti^{3+} into $Na_2Ti_3O_7$ increases both ion and electron conductivity as a high-performance anode material for sodium-ion batteries, *J. Alloys Compd.*, 2018, **767**, 820–828.

54 Z. Zhou, H. Xiao, F. Zhang, X. Zhang and Y. Tang, Solvothermal synthesis of $Na_2Ti_3O_7$ nanowires embedded in 3D graphene networks as an anode for high-performance sodium-ion batteries, *Electrochim. Acta*, 2016, **211**, 430–436.

55 Z. Li, S. Ye, W. Wang, Q. Xu, H. Liu and Y. Wang, *et al.*, Free-Standing Sandwich-Structured Flexible Film Electrode Composed of $Na_2Ti_3O_7$ Nanowires@CNT and Reduced Graphene Oxide for Advanced Sodium-Ion Batteries, *ACS Omega*, 2017, **2**(9), 5726–5736.

56 R. Bi, C. Zeng, T. Ma, A. Etogo, X. Wang and L. Zhang, Encapsulated hollow $Na_2Ti_3O_7$ spheres in reduced graphene oxide films for flexible sodium-ion batteries, *Electrochim. Acta*, 2018, **284**, 287–293.

57 S. Chandel, Zulkifli, J. Singh, J. Kim and A. K. Rai, Reduced graphene oxide (rGO) integrated sodium titanate nanocomposite as a high-rate performance anode material for sodium ion batteries, *J. Electroanal. Chem.*, 2023, **939**, 117485.

58 J. Wang, J. Bi, W. Wang, Z. Xing, Y. Bai and M. Leng, *et al.*, $Na_2Ti_6O_{13}$ Coated with Carbon Produced by Citric Acid as an Anode Material in Sodium Ion Batteries, *J. Electrochem. Soc.*, 2020, **167**(9), 090539.

59 P. L. M. Kanta, M. Venkatesh, S. K. Yadav, B. K. Das and R. Gopalan, Scalable Synthesis and Kinetic Studies of Carbon Coated Sodium Titanate: A Promising Ultra-low Voltage Anode for Sodium Ion Battery, *Trans. Indian Natl. Acad. Eng.*, 2020, **5**(3), 475–483.

60 A. Mukherjee, D. Das, S. Banerjee and S. B. Majumder, Synthesis and electrochemical performance of in situ and ex situ carbon-coated $Na_2Ti_3O_7$, as a promising anode for sodium-ion batteries. Electrochem, *Sci. Adv.*, 2023, **3**(5), 1–13.

61 A. Mukherjee, S. Mondal, D. Das, S. Banerjee and S. B. Majumder, Surface modified sodium titanate as low voltage anode for sodium rechargeable cell with superior electrochemical properties, *Mater. Lett.*, 2021, **301**, 130219.

62 J. Liu, Z. Wang, Z. Lu, L. Zhang, F. Xie and A. Vasileff, *et al.*, Efficient Surface Modulation of Single-Crystalline $Na_2Ti_3O_7$Nanotube Arrays with Ti^{3+} Self-Doping toward Superior Sodium Storage, *ACS Mater. Lett.*, 2019, **1**(4), 389–398.

63 D. Kong, Y. Wang, S. Huang, Y. V. Lim, J. Zhang and L. Sun, *et al.*, Surface Modification of $Na_2Ti_3O_7$ Nanofibre Arrays by N-doped Graphene Quantum Dots as Advanced Anodes for Sodium-ion Batteries with Ultra-stable and High-rate Capability, *J. Mater. Chem. A*, 2019, **7**(20), 12751–12762.

64 X. Wang, Y. Li, Y. Gao, Z. Wang and L. Chen, Additive-free sodium titanate nanotube array as advanced electrode for sodium ion batteries, *Nano Energy*, 2015, **13**, 687–692.

65 Y. Ge, J. Zhu, M. Dirican, H. Jia, M. Yanilmaz and Y. Lu, *et al.*, Fabrication and electrochemical behavior study of nano-fibrous sodium titanate composite, *Mater. Lett.*, 2017, **188**, 176–179.

66 S. Anwer, Y. Huang, J. Liu, J. Liu and M. Xu, Nature Inspired $Na_2Ti_3O_7$ Nanosheets Formed Three-Dimensional Micro-Flowers Architecture as a High-Performance Anode Material for Rechargeable Sodium Ion Batteries, *ACS Appl. Mater. Interfaces*, 2017, **9**(13), 11669–11677.

67 Q.-S. Lai, J.-J. Mu, Z.-M. Liu, L.-K. Zhao, X.-W. Gao and D.-R. Yang, *et al.*, Tunnel-Type $Na_2Ti_6O_{13}$@Carbon Nanowires as Anode Materials for Low-Temperature Sodium-Ion Batteries, *Batteries Supercaps*, 2023, **6**(4), e202200549.

68 Q. Xia, Y. Liang, E. R. Cooper, C. Ko, Z. Hu and W. Li, *et al.*, Monolayer Sodium Titanate Nanobelts as a Highly Efficient Anode Material for Sodium-Ion Batteries, *Adv. Energy Mater.*, 2024, **14**, 2400929.

69 A. Sarkar, C. V. Manohar and S. Mitra, A simple approach to minimize the first cycle irreversible loss of sodium titanate anode towards the development of sodium-ion battery, *Nano Energy*, 2020, **70**, 104520.

70 S. Chandel, C. Wang, S. P. Singh, N. Wang and A. K. Rai, Significant Enhancement in the Electrochemical Performances of a Nanostructured Sodium Titanate Anode by Molybdenum Doping for Applications as Sodium-Ion Batteries, *ACS Appl. Nano Mater.*, 2022, **5**(12), 18591–18602.

71 S. Chandel, N. Zulkifli, J. Kim and A. K. Rai, Effect of vanadium doping on the electrochemical performances of sodium titanate anode for sodium ion battery application, *Dalton Trans.*, 2022, **51**(31), 11797–11805.

72 D. P. Opra, V. V. Zheleznov, S. L. Sinebryukhov, A. A. Sokolov, A. M. Ziatdinov and A. B. Podgorbunsky, *et al.*, Copper-doped sodium titanate with a hierarchical micro/nano structure as an anode material for Na-ion batteries, *J. Power Sources*, 2024, **600**, 234230.

73 F. Li, L. Gao, Y. Lv, B. Cai, C. Wang and X. S. Zhao, Doping of potassium by partial substitution of sodium in sodium trititanate for improved sodium-ion storage properties, *J. Power Sources*, 2024, **623**, 235393.

74 Z. Yan, L. Liu, H. Shu, X. Yang, H. Wang and J. Tan, *et al.*, A tightly integrated sodium titanate-carbon composite as an anode material for rechargeable sodium ion batteries, *J. Power Sources*, 2015, **274**, 8–14.

75 Z. Li, Y. Huang, Y. Jiang, Z. Wang, B. Lu and J. Zhou, *et al.*, Dense Sandwich-like $Na_2Ti_3O_7$@rGO Composite with Superior Performance for Sodium Storage, *ChemElectroChem*, 2020, **7**(10), 2258–2264.

76 J. Song, J. Han, H. C. Ju, H. A. Seo, B. Yun and D. Moon, *et al.*, A Sandwich-Structured $Na_2Ti_6O_{13}$/Reduced Graphene Oxide Composite for Improved Energy Storage in Sodium-Ion Batteries, *Small Methods*, 2025, **10**(2), 2500671.

77 M. Li, X. Xiao, X. Fan, X. Huang, Y. Liu and L. Chen, Carbon coated sodium-titanate nanotube as an advanced intercalation anode material for sodium-ion batteries, *J. Alloys Compd.*, 2017, **712**, 365–372.

78 F. Xie, L. Zhang, D. Su, M. Jaroniec and S.-Z. Qiao, $Na_2Ti_3O_7$@N-doped Carbon Hollow Spheres for Sodium-Ion Batteries with Excellent Rate Performance, *Adv. Mater.*, 2017, **29**(24), 1700989.

79 J. Hwang, H. Setiadi Cahyadi, W. Chang and J. Kim, Uniform and ultrathin carbon-layer coated layered $Na_2Ti_3O_7$ and tunnel $Na_2Ti_6O_{13}$ hybrid with enhanced electrochemical performance for anodes in sodium ion batteries, *J. Supercrit. Fluids*, 2019, **148**, 116–129.

80 D. Ba, W. Zhu and Y. Li, Synergistically enhancing cycleability and rate performance of sodium titanate nanowire anode via hydrogenation and carbon coating for advanced sodium ion batteries, *Rare Met.*, 2022, **41**(12), 4075–4085.

81 W. Zhong, M. Tao, W. Tang, W. Gao, T. Yang and Y. Zhang, *et al.*, MXene-derivative pompon-like $Na_2Ti_3O_7$@C anode material for advanced sodium ion batteries, *Chem. Eng. J.*, 2019, **378**, 122209.

82 X. Yin, L. Zhu, Y. Zhang, X. Yang and L. Xie, Sodium Titanate Nanorods Decorated with Silver Nanoparticles as a High-Performance Anode Material for Sodium-Ion Batteries, *Electrochim. Acta*, 2023, **469**, 143226.

83 J. Mei, T. Wang, D. Qi, J. Liu, T. Liao and Y. Yamauchi, *et al.*, Three-Dimensional Fast Na-Ion Transport in Sodium Titanate Nanoarchitectures via Engineering of Oxygen Vacancies and Bismuth Substitution, *ACS Nano*, 2021, **15**(8), 13604–13615.